

Supporting Information

Developing a series of calcium-doped pyrochlore iridates for the oxygen evolution reaction in PEM water electrolysis

Felix Kerner,^a Kohei Miyazaki^{b,c} and Daniel Schröder^{*a,d}

^a Technische Universität Braunschweig, Institute of Energy and Process Systems Engineering (InES), Langer Kamp 19B, 38106 Braunschweig, Germany

^b Kyoto University, Graduate School of Engineering, Kyoto 615-8510, Japan

^c Kobe University, Graduate School of Engineering, Kobe 657-8501, Japan

^d Technische Universität Braunschweig, Battery LabFactory Braunschweig (BLB), Langer Kamp 19, 38106 Braunschweig, Germany

X-ray fluorescence (XRF) analysis

Several elements could not be excluded from the measurement. Since especially phosphorous had a large wt% (likely originating from the sample holder materials), the weight percentages measured by the device do not represent the real wt% of the metals in the sample. To account for this, the measured weight percentages of the three metals were put into relation of their sum, excluding the weight percentages of the other elements.

$$wt\%(metal)_{meas} = \frac{wt\%(metal)_{XRF}}{wt\%(Pr)_{XRF} + wt\%(Ca)_{XRF} + wt\%(Ir)_{XRF}} \cdot 100 \%$$

$$wt\%(Pr)_{theo} = \frac{(2-x) \cdot M(Pr)}{(2-x) \cdot M(Pr) + x \cdot M(Ca) + 2 \cdot M(Ir)} \cdot 100 \%$$

$$wt\%(Ca)_{theo} = \frac{x \cdot M(Ca)}{(2-x) \cdot M(Pr) + x \cdot M(Ca) + 2 \cdot M(Ir)} \cdot 100 \%$$

$$wt\%(Ir)_{theo} = \frac{2 \cdot M(Ir)}{(2-x) \cdot M(Pr) + x \cdot M(Ca) + 2 \cdot M(Ir)} \cdot 100 \%$$

Brunauer-Emmett-Teller (BET) analysis

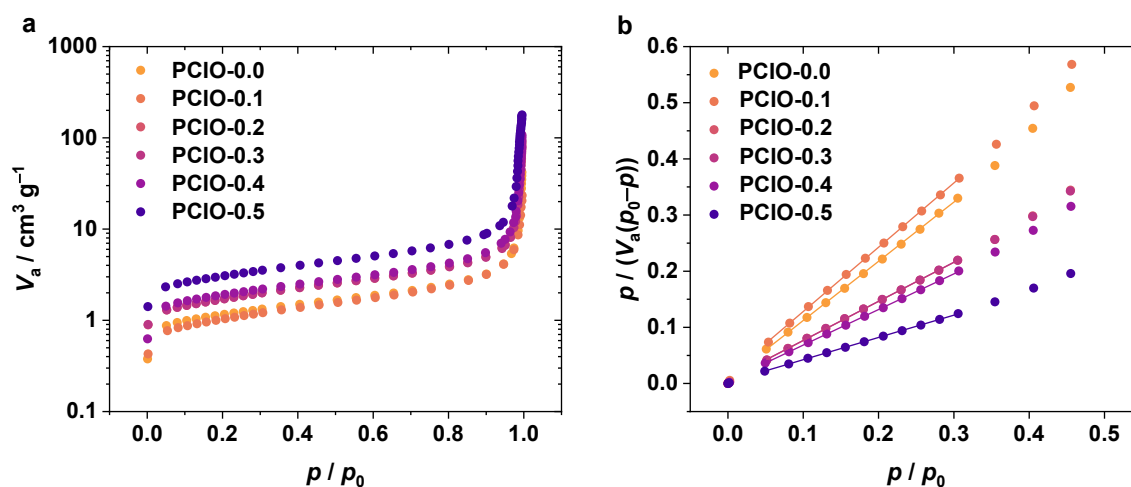
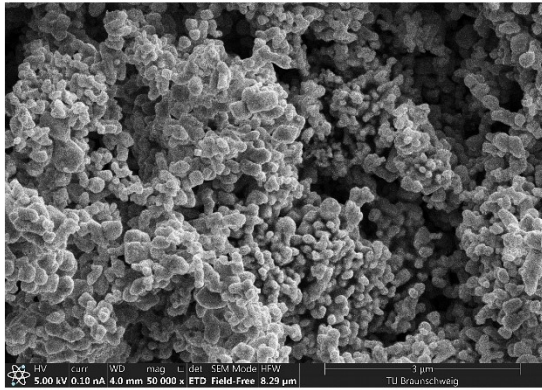


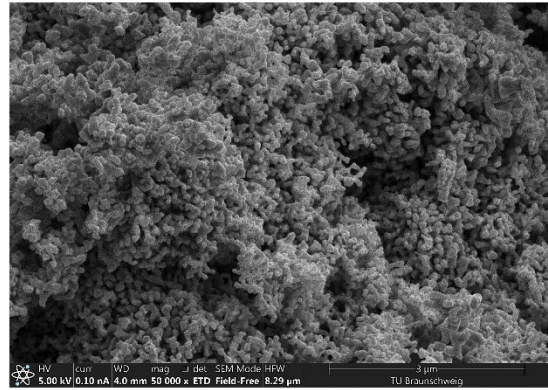
Figure S 1: Nitrogen adsorption isotherms (a) and BET analysis (b).

Scanning electron microscopy (SEM) images

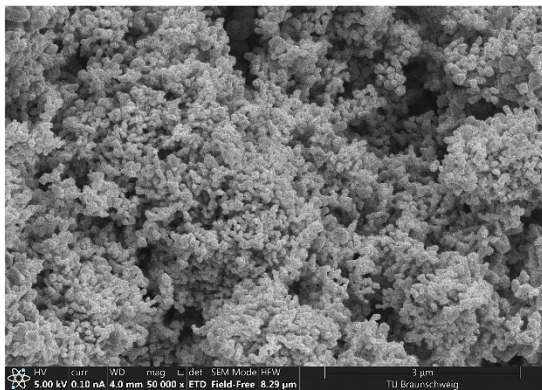
a



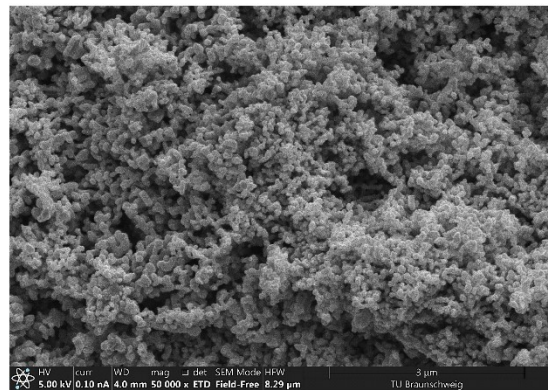
b



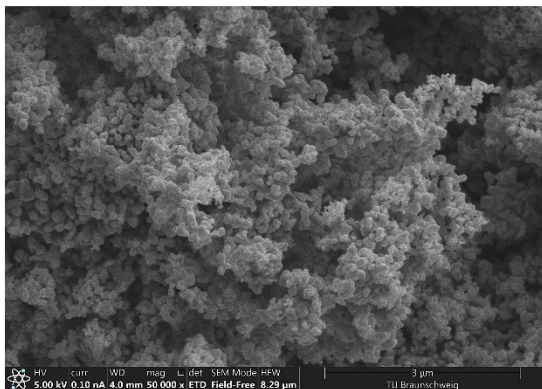
c



d



e



f

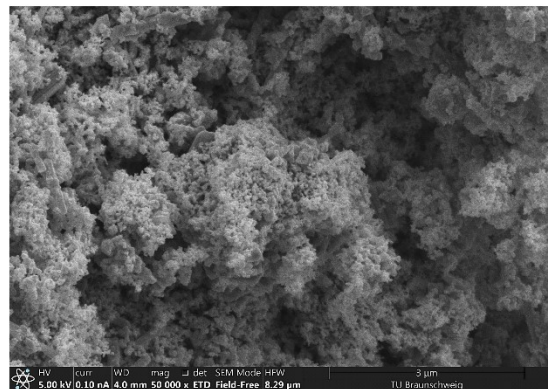
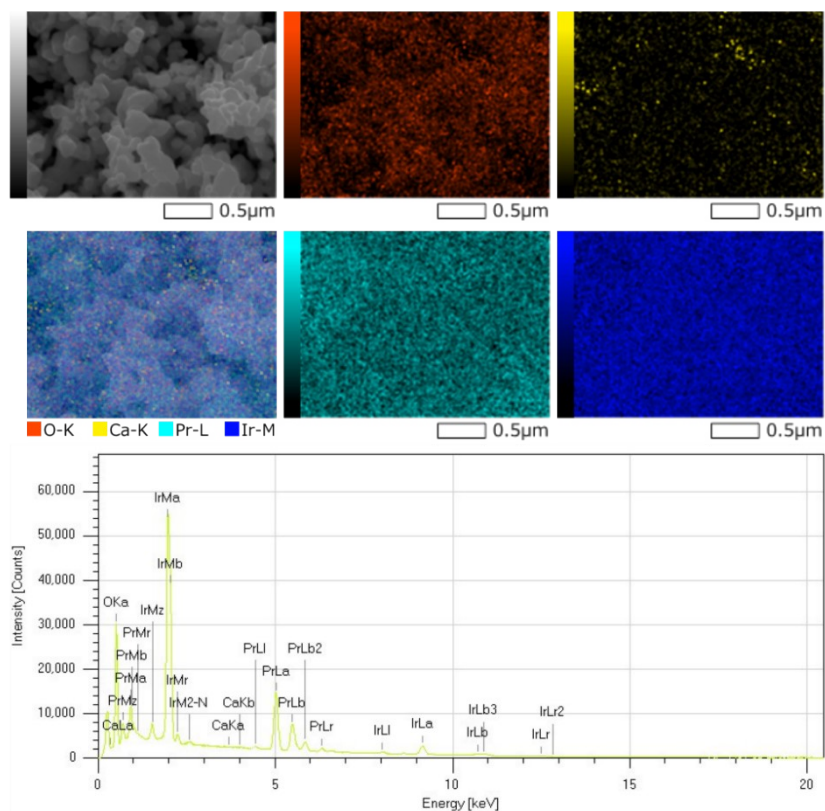


Figure S 2: SEM images of the PCIO materials: a) PCIO-0.0, b) PCIO-0.1, c) PCIO-0.2, d) PCIO-0.3, e) PCIO-0.4, f) PCIO-0.5.

SEM energy dispersive X-ray spectroscopy (SEM-EDX) images

a



b

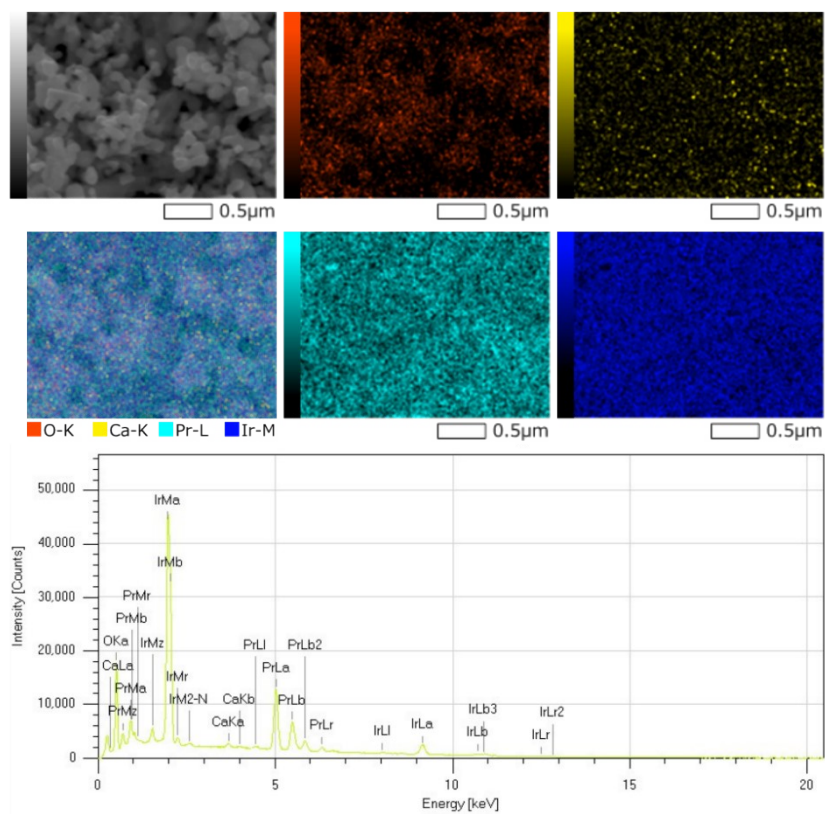
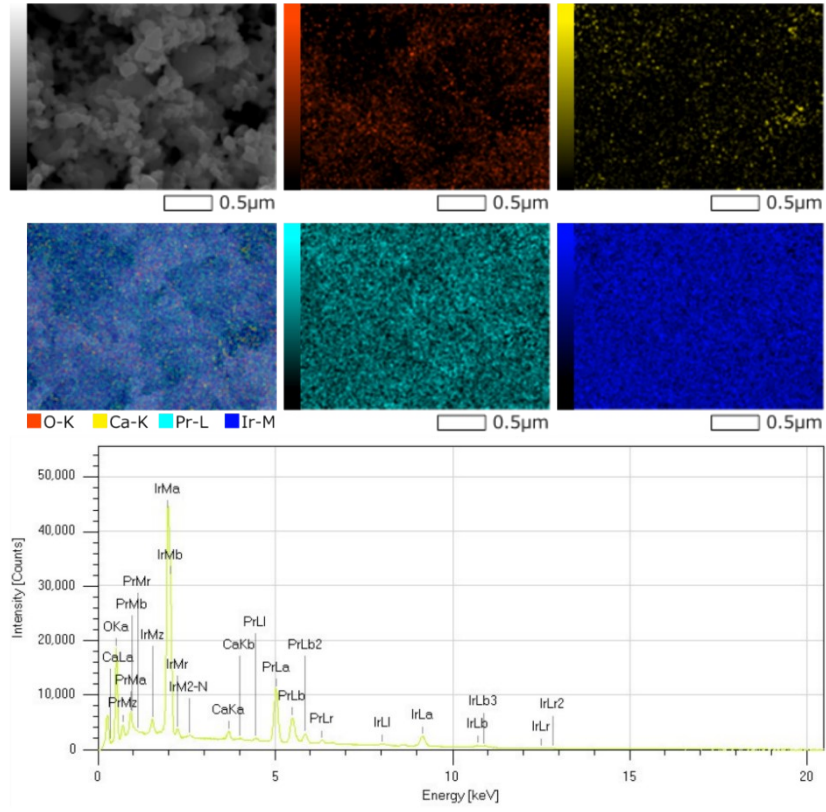
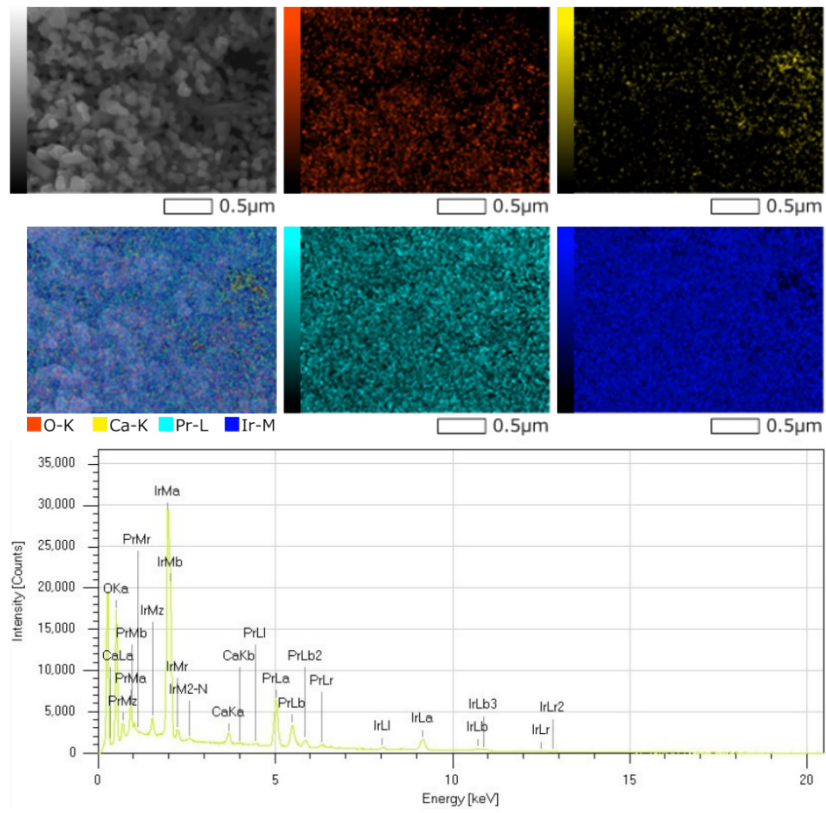
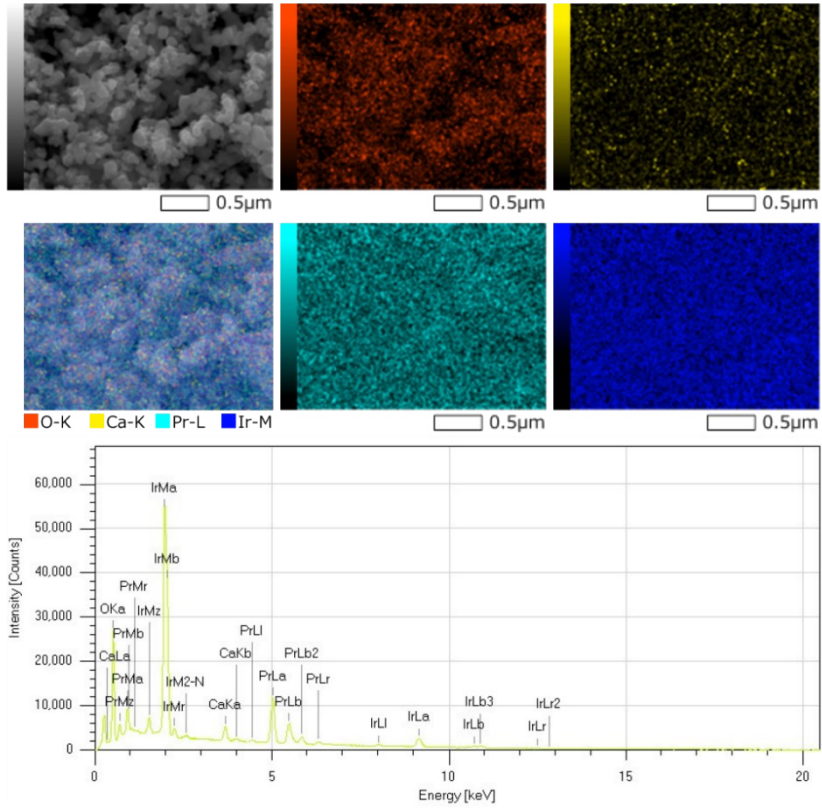
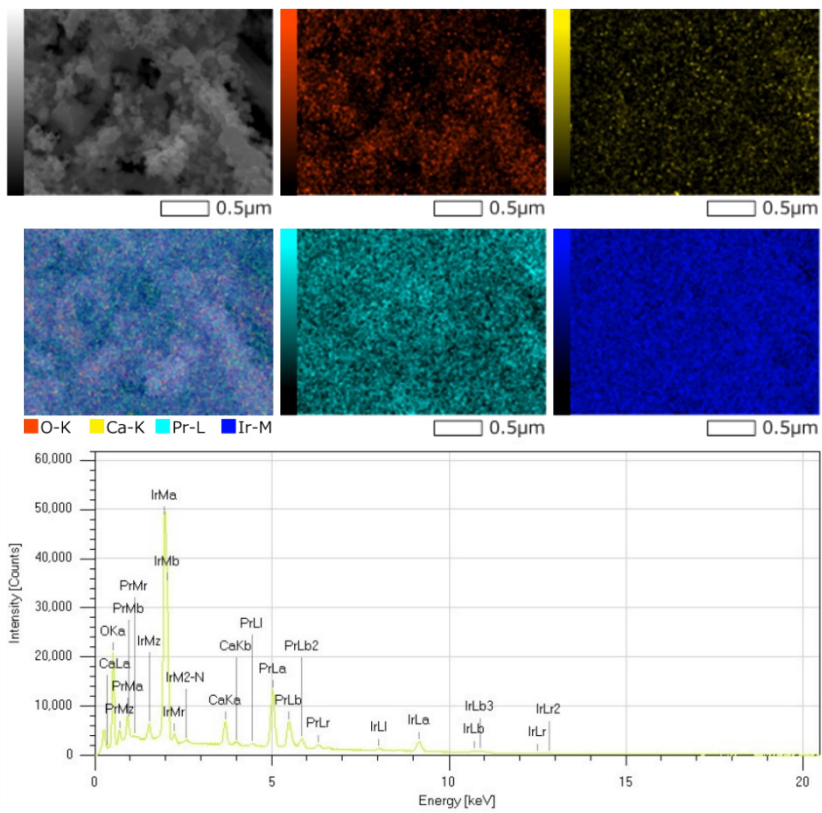


Figure S 3: SEM-EDX elemental mapping and intensities: a) PCIO-0.0, b) PCIO-0.1, c) PCIO-0.2, d) PCIO-0.3, e) PCIO-0.4, f) PCIO-0.5. Elemental distribution maps are presented with ZAF correction applied. For PCIO-0.0, the CaK α signal can barely discriminated from the background, so the elemental mapping represents only traces of Ca in the sample.

c**d****Figure S 3: (Continued.)**

e**f****Figure S 3: (Continued.)**

X-ray Photoelectron Spectroscopy (XPS) spectra of Ir 4f region

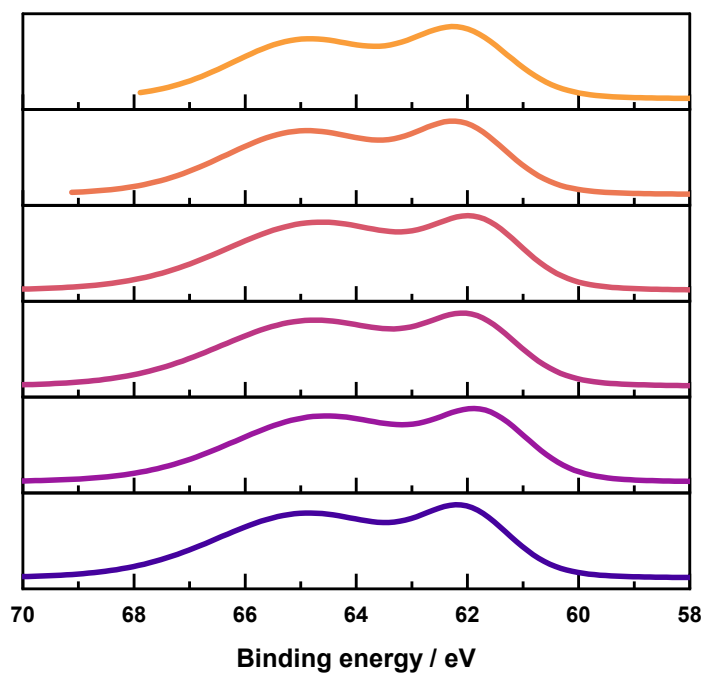


Figure S 4: High-resolution XPS spectrum of the Ir 4f region

Determination of the electrochemically active surface area (ECSA)

The electrochemically active surface area was determined by measuring cyclic voltammograms at different scan rates in the non-Faradaic region. The modulus of the current was averaged between forward and backward scan and plotted against the scan rate. The ECSA was determined from the double layer capacity given by the slope, the catalyst loading of $m_{\text{cat}} = 50 \mu\text{g}$ and the specific capacitance usually given as $C_s = 60 \mu\text{F}/\text{cm}^2$.^{1,2}

$$ECSA = \frac{C_{DL}}{C_s \cdot m_{cat}}$$

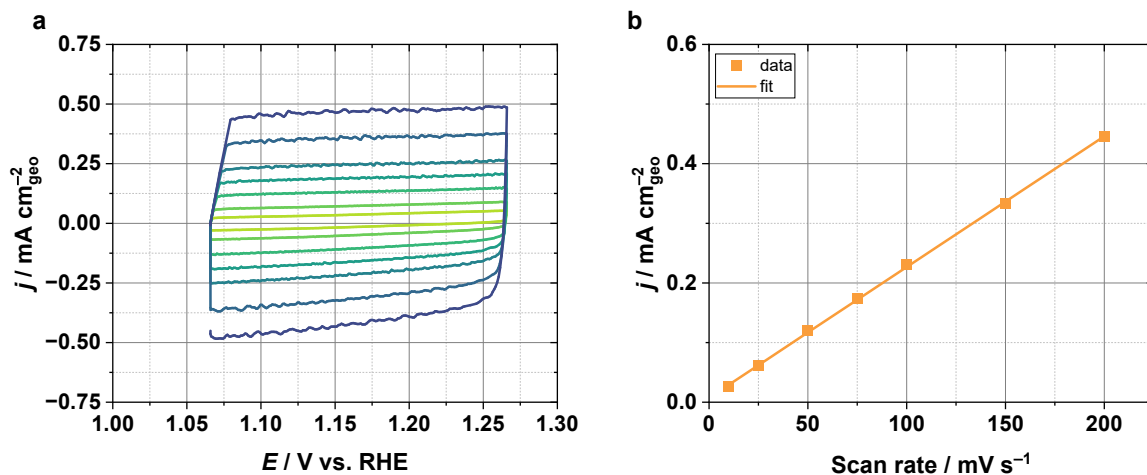


Figure S 5: ECSA determination of PCIO-0.0: a) CVs at different scan rates in non-Faradaic region, b) charging current density at 1.166 V vs. RHE (0.90 V vs. Ag/AgCl 3M KCl) against scan rate.

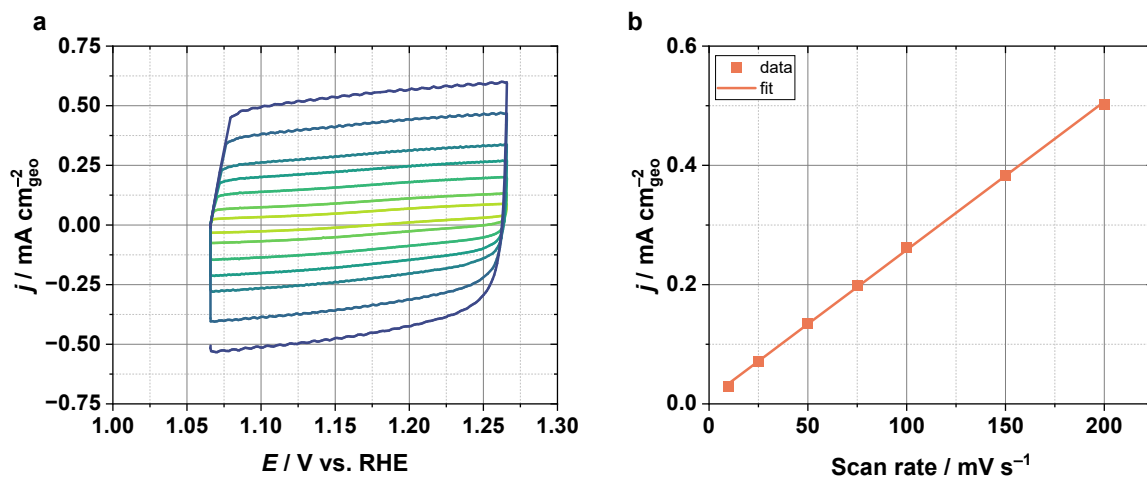


Figure S 6: ECSA determination of PCIO-0.1: a) CVs at different scan rates in non-Faradaic region, b) charging current density at 1.166 V vs. RHE (0.90 V vs. Ag/AgCl 3M KCl) against scan rate.

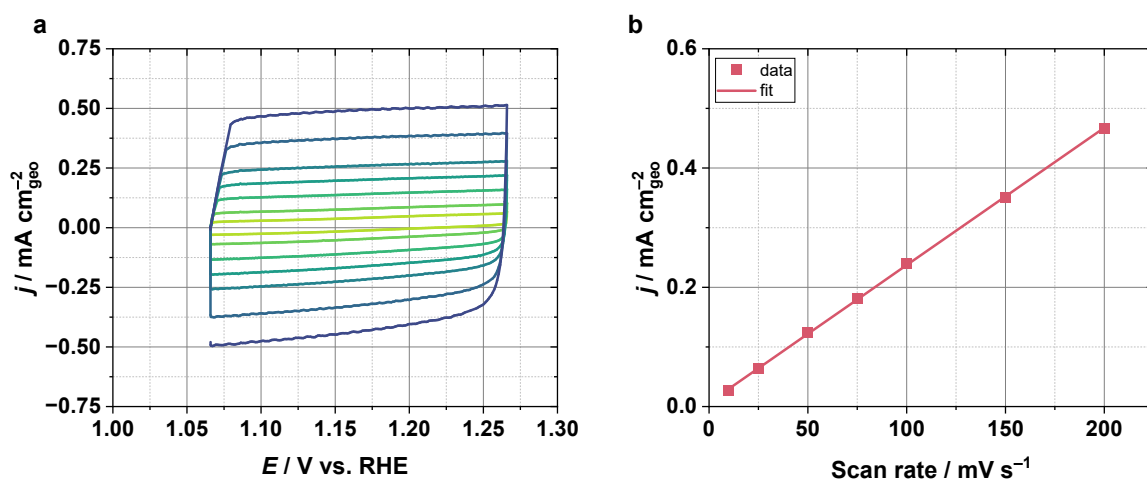


Figure S 7: ECSA determination of PCIO-0.2: a) CVs at different scan rates in non-Faradaic region, b) charging current density at 1.166 V vs. RHE (0.90 V vs. Ag/AgCl 3M KCl) against scan rate.

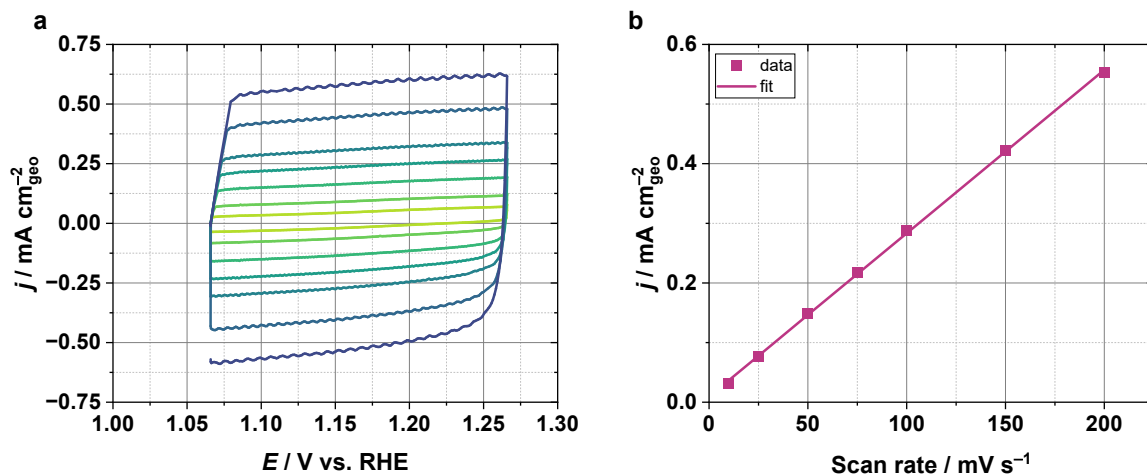


Figure S 8: ECSA determination of PCIO-0.3: a) CVs at different scan rates in non-faradaic region, b) charging current density at 1.166 V vs. RHE (0.90 V vs. Ag/AgCl 3M KCl) against scan rate.

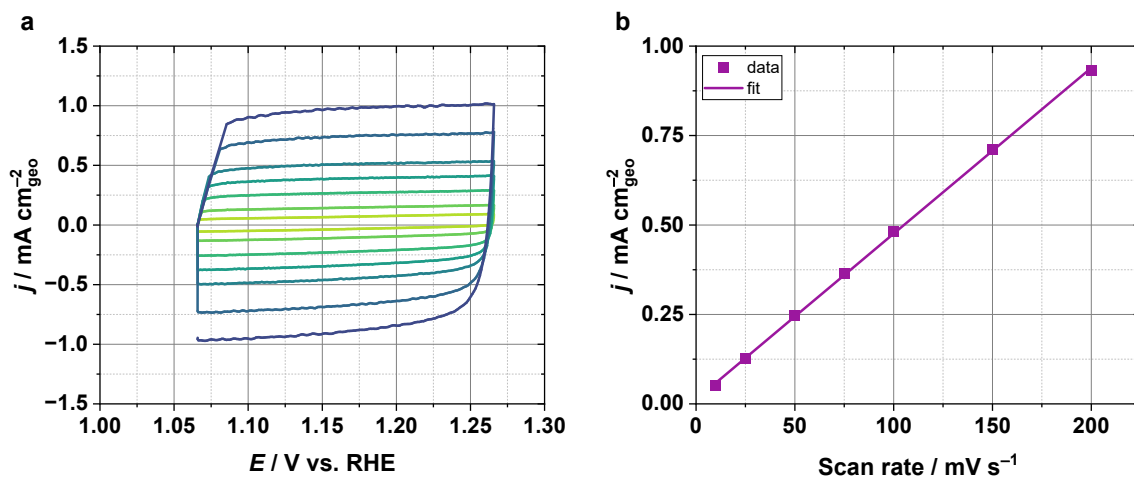


Figure S 9: ECSA determination of PCIO-0.4: a) CVs at different scan rates in non-Faradaic region, b) charging current density at 1.166 V vs. RHE (0.90 V vs. Ag/AgCl 3M KCl) against scan rate.

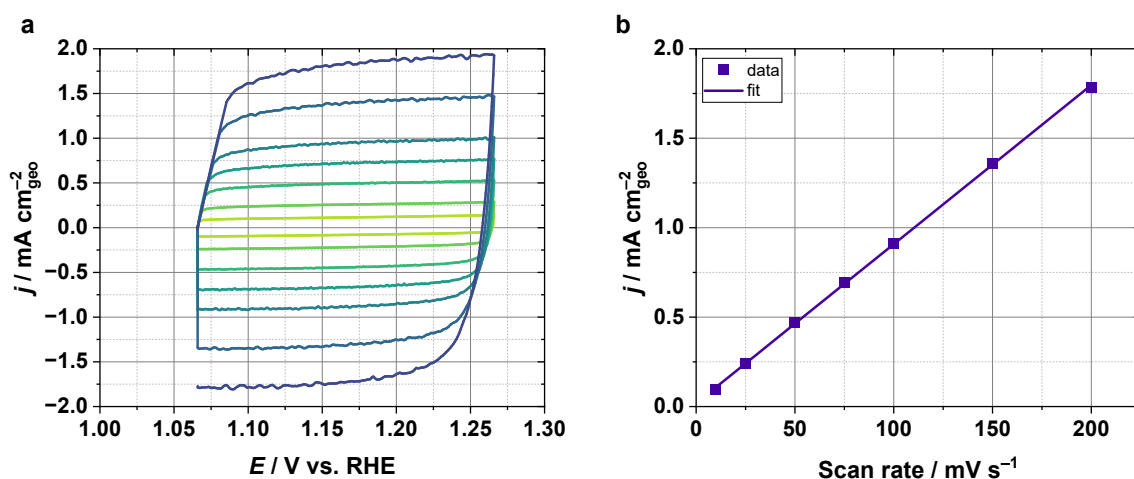


Figure S 10: ECSA determination of PCIO-0.5: a) CVs at different scan rates in non-Faradaic region, b) charging current density at 1.166 V vs. RHE (0.90 V vs. Ag/AgCl 3M KCl) against scan rate.

Determination of the S-number

The stability number was determined by assuming 100 % Faradaic efficiency. The amount of oxygen evolved was calculated from the charge transferred during the 10 cyclovoltammetry cycles as well as the 60 min chrono potentiometric holds. The amount of iridium dissolved was determined via ICP-MS. Shown below is an exemplary calculation for PCIO-0.5.

$$n_{O_2}^{evolved} = \frac{\int_0^t i dt}{Fn} = \frac{1.051 C (from CV) + 1.963 mA \cdot 3600 s (from CP)}{96485 \frac{C}{mol} \cdot 4} = 2.103 \cdot 10^{-5} mol$$

$$n_{Ir}^{dissolved} = \frac{c_{Ir} \cdot V}{M_{Ir}} = \frac{10.82 \mu g/L \cdot 0.0090 L}{192.217 g/mol} = 5.065 \cdot 10^{-10} mol$$

$$S - number = \frac{n_{O_2}^{evolved}}{n_{Ir}^{dissolved}} = \frac{2.103 \cdot 10^{-5} mol}{5.065 \cdot 10^{-10} mol} = 4.15 \cdot 10^4$$

Table S 1: Comparison of environment, electrolyte, testing conditions and ionomer content for the S-numbers of catalysts compared within this work.

Reference	Environment	Electrolyte	Catalyst	Testing conditions	Ionomer content	S-number
Geiger et al. ³	SFC	0.1 M HClO ₄	IrO ₂	5 mV/s sweep to 1.8 V	4.3 wt%	~2.0 · 10 ⁶
Geiger et al. ³	SFC	0.1 M HClO ₄	IrO _x	5 mV/s sweep to 1.65 V	40.5 wt%	~1.0 · 10 ⁵
Geiger et al. ³	SFC	0.1 M HClO ₄	Ir metal	5 mV/s sweep to 1.55 V	40.5 wt%	~1.0 · 10 ⁵
Geiger et al. ³	SFC	0.1 M HClO ₄	Ba ₂ PrlrO ₆	5 mV/s sweep to 1.65 V	40.5 wt%	~3.0 · 10 ⁴
Chen et al. ⁴	RDE	0.1 M HClO ₄	IrO ₂	10 mA/cm _{geo} ² 180 min	14 wt%	~1.0 · 10 ⁵
Chen et al. ⁴	RDE	0.1 M HClO ₄	Ir metal	10 mA/cm _{geo} ² 180 min	14 wt%	~5.0 · 10 ⁴
Chen et al. ⁴	RDE	0.1 M HClO ₄	SrCo _{0.9} Ir _{0.1} O _{3.6}	10 mA/cm _{geo} ² 180 min	14 wt%	~8.0 · 10 ⁴
Edgington et al. ⁵	Steady state cell	0.1 M HClO ₄	IrO _x	20 mV/s sweep to 1.7 V 1.7 V hold 10 min 20 mV/s sweep to OCV repeat	8 – 16 wt%	2.3 · 10 ⁵
Edgington et al. ⁵	Steady state cell	0.1 M HClO ₄	SrIr _{0.8} Zn _{0.2} O ₃	20 mV/s sweep to 1.7 V 1.7 V hold 10 min 20 mV/s sweep to OCV repeat	8 – 16 wt%	3.2 · 10 ⁵
Zhang et al. ⁶	Steady state cell	0.1 M HClO ₄	H _{3.6} IrO ₄ · 3.7 H ₂ O	1 mA/cm _{oxide} ² (15 mA/cm _{geo} ²) 60 min	N/A	~1.5 · 10 ⁵
Zhang et al. ⁶	Steady state cell	0.1 M HClO ₄	H _{3.5} IrO ₄	1 mA/cm _{oxide} ² (11 mA/cm _{geo} ²) 60 min	N/A	~1.3 · 10 ⁵
Zhang et al. ⁶	Steady state cell	0.1 M HClO ₄	6H-SrIrO ₃	1 mA/cm _{oxide} ² (5 mA/cm _{geo} ²) 60 min	N/A	~2.2 · 10 ⁴
Zhang et al. ⁶	Steady state cell	0.1 M HClO ₄	Sr ₂ Ir _{0.5} Fe _{0.5} O ₄	1 mA/cm _{oxide} ² (3.5 mA/cm _{geo} ²) 60 min	N/A	~2.0 · 10 ³
This work	RDE	0.1 M HClO ₄	PCIO-0.0	10 x 20 mV/s cycling (1.066 – 1.766 V) 10 mA/cm _{geo} ² 60 min	14 wt%	1.81 · 10 ⁴
This work	RDE	0.1 M HClO ₄	PCIO-0.1	10 x 20 mV/s cycling (1.066 – 1.766 V) 10 mA/cm _{geo} ² 60 min	14 wt%	1.80 · 10 ⁴
This work	RDE	0.1 M HClO ₄	PCIO-0.2	10 x 20 mV/s cycling (1.066 – 1.766 V) 10 mA/cm _{geo} ² 60 min	14 wt%	2.62 · 10 ⁴
This work	RDE	0.1 M HClO ₄	PCIO-0.3	10 x 20 mV/s cycling (1.066 – 1.766 V) 10 mA/cm _{geo} ² 60 min	14 wt%	3.12 · 10 ⁴
This work	RDE	0.1 M HClO ₄	PCIO-0.4	10 x 20 mV/s cycling (1.066 – 1.766 V) 10 mA/cm _{geo} ² 60 min	14 wt%	3.56 · 10 ⁴
This work	RDE	0.1 M HClO ₄	PCIO-0.5	10 x 20 mV/s cycling (1.066 – 1.766 V) 10 mA/cm _{geo} ² 60 min	14 wt%	4.15 · 10 ⁴

References

- 1 O. Diaz-Morales, S. Raaijman, R. Kortlever, P. J. Kooyman, T. Wezendonk, J. Gascon, W. T. Fu, M. T. M. Koper, *Nat. Commun.* 2016, **7**, 10.1038/ncomms12363.
- 2 C. Shang, C. Cao, D. Yu, Y. Yan, Y. Lin, H. Li, T. Zheng, X. Yan, W. Yu, S. Zhou, J. Zeng, *Adv. Mater.* 2019, **31**, 1805104.

- 3 S. Geiger, O. Kasian, M. Ledendecker, E. Pizzutilo, A. M. Mingers, W. T. Fu, O. Diaz-morales, Z. Li, T. Oellers, L. Fruchter, A. Ludwig, K. J. J. Mayrhofer, M. T. M. Koper, S. Cherevko, *Nat. Catal.* 2018, **1**, 508–515.
- 4 Y. Chen, H. Li, J. Wang, Y. Du, S. Xi, Y. Sun, M. Sherburne, J. W. Ager, A. C. Fisher, Z. J. Xu, *Nat. Commun.* 2019, **10**, 10.1038/s41467-019-08532-3.
- 5 J. Edgington, A. Deberghes, L. C. Seitz, *ACS Appl. Energy Mater.* 2022, **5**, 12206–12218.
- 6 R. Zhang, P. E. Pearce, V. Pimenta, J. Cabana, H. Li, D. Alves Dalla Corte, A. M. Abakumov, G. Rousse, D. Giaume, M. Deschamps, A. Grimaud, *Chem. Mater.* 2020, **32**, 3499–3509.